# A Disposable Carbon-Based Electrochemical Cell Modified With Carbon Black and Ag/δ-FeOOH for Non-enzymatic H2O2 Electro-Chemical Sensing

Wiviane Reis , Karoline Nantes , Ana Ferreira , Márcio Pereira , Luiz Mattoso , Ronaldo Faria , Andre Afonso *

Posted Date: 10 October 2023

doi: 10.20944/preprints202310.0476.v1

Keywords: non-enzymatic sensor; Ag/δ-FeOOH; carbon black; hydrogen peroxide; electrochemical detection

*Article*

# A Disposable Carbon-Based Electrochemical Cell Modified with Carbon Black and Ag/δ-FeOOH for Non-Enzymatic $H_2O_2$ Electrochemical Sensing

**Wiviane E. Reis [1], Karoline S. Nantes [1], Ana L. H. K. Ferreira [1], Márcio C. Pereira [1], Luiz H. C. Mattoso [2], Ronaldo C. Faria [3] and André S. Afonso [1,*]**

[1] Institute of Science, Engineering, and Technology, Federal University of Jequitinhonha and Mucuri Valleys,Teófilo Otoni 39803-371, Minas Gerais, Brazil.
[2] Nanotechnology National Laboratory for Agriculture (LNNA), Embrapa Instrumentação, São Carlos, 13560-970, São Paulo, Brazil.
[3] Chemistry Department, Federal University of São Carlos, CP 676, São Carlos 13565-905, São Paulo, Brazil.
* Correspondence: andre.afonso@ufvjm.edu.br

**Abstract:** Hydrogen peroxide ($H_2O_2$) is an essential analyte for detecting neurodegenerative diseases and inflammatory processes and plays a crucial role in pharmaceutical, food industry, and environmental monitoring. However, conventional $H_2O_2$ detection methods have drawbacks such as lengthy analysis time, high costs, and bulky equipment. Non-enzymatic sensors have emerged as promising alternatives to overcome these limitations. In this study, we introduce a simple, portable, and cost-effective non-enzymatic electrochemical sensor based on carbon black (CB) and silver nanoparticle-modified δ-FeOOH (Ag/δ-FeOOH), integrated into a disposable electrochemical cell (DCell). Scanning electron microscopy (SEM), energy-dispersive X-ray spectroscopy (EDS), and electrochemical impedance spectroscopy (EIS), confirmed successful CB and Ag/δ-FeOOH immobilization on the DCell working electrode. Electrochemical investigations revealed that the DCell-CB//Ag/δ-FeOOH sensor exhibited an approximately twofold higher apparent heterogeneous electron transfer rate constant than the DCell–Ag/δ-FeOOH sensor, capitalizing on CB advantages. Moreover, the sensor displayed excellent electrochemical response for $H_2O_2$ reduction, boasting a low detection limit of 22 μM and a high analytical sensitivity of 214 μA $mM^{-1}$ $cm^{-2}$. Notably, the DCell-CB//Ag/δ-FeOOH sensor exhibited outstanding selectivity for $H_2O_2$ detection, even in potential interferents such as dopamine, uric acid, and ascorbic acid. Furthermore, the sensor demonstrated its suitability for monitoring $H_2O_2$ in complex biological samples, as evidenced by $H_2O_2$ recoveries ranging from 92% to 103% in 10% fetal bovine serum. These findings underscore the considerable potential of the DCell-CB//Ag/δ-FeOOH sensor for precise and reliable $H_2O_2$ monitoring in diverse biomedical and environmental applications.

**Keywords:** Non-enzymatic sensor, Ag/δ-FeOOH, carbon black, hydrogen peroxide, electrochemical detection.

## 1. Introduction

The medical community is dedicated to early disease detection and prevention using new therapies and technologies, considerably improving quality of life and life expectancy, especially for individuals with early signs of cancer or neurodegenerative diseases like Parkinson's or Alzheimer's[1,2]. These conditions share a common role played by reactive oxygen species (ROS), which are generated through the redox reaction of oxygen-containing molecules such as superoxide ($O_2^{\bullet-}$), hydroxyl (•OH), peroxyl radical (ROO•), and hydrogen peroxide ($H_2O_2$) [3]. While ROS are naturally produced during normal cellular processes, their concentration tends to rise in certain disease states or chronic inflammation due to cellular metabolism changes. Hydrogen peroxide, among the ROS, has been investigated as a disease indicator, with $H_2O_2$ levels in human blood ranging from 30 to 50 μM[4]. Additionally, $H_2O_2$ is a by-product of enzyme-catalyzed reactions, enabling the determination of various biological substances such as cholesterol, glucose, lactate, and urate through $H_2O_2$ analysis [5].

Accurate measurement of $H_2O_2$ is crucial in pharmaceutical, food sterilization, and environmental monitoring industries. Various techniques, including titration, spectrophotometry,

 doi:10.20944/preprints202310.0476.v1



chemiluminescence, fluorescence, and chromatography, have been employed for $H_2O_2$ detection and quantification. However, these methods often suffer from drawbacks such as high costs, lengthy analysis time, and bulky equipment. In contrast, electrochemical methods offer a more advantageous alternative due to their affordability, portability, miniaturization capability, rapid response, reproducibility, and high sensitivity. Effective $H_2O_2$ detection can be achieved by modifying electrodes with nanostructured materials, ensuring high sensitivity and reproducibility[4] .

In electrochemical sensors for $H_2O_2$ determination, both enzymatic and non-enzymatic approaches have been developed for applications in biological and environmental settings. Enzymatic sensors, despite their widespread use, face challenges like enzyme activity loss due to temperature and pH variations, high costs, and difficulties in proper enzyme immobilization. On the other hand, non-enzymatic sensors offer desirable features such as stability and low cost[6]. Researchers have successfully designed sensors with $H_2O_2$ sensing capabilities using non-enzymatic metal oxide/hydroxide materials. Recently, an all-plastic disposable carbon electrochemical cell modified with silver nanoparticles and δ-FeOOH has been developed, demonstrating excellent electrocatalytic response for $H_2O_2$ reduction, with a detection limit of 71 μM[7]. δ-FeOOH, one of the stable phases of iron oxyhydroxide, holds significant potential for various applications, including water treatment, organic pollutant degradation, solar cells, and photocatalysis [8]. While several researchers have explored non-enzymatic sensors using different iron oxyhydroxide phases[9-12], the utilization of δ-FeOOH in non-enzymatic sensors has been limited.

On the other hand, carbon-based nanomaterials have been extensively utilized to enhance the electrochemical properties of non-enzymatic sensors. These nanomaterials possess intrinsic advantages such as a large surface area and $sp^2$ carbon structure, resulting in increased electroactive area and enhanced electron transfer rate[13]. Carbon black (CB) is particularly advantageous among these nanomaterials due to its affordability, high electrical conductivity, and signal amplification capabilities similar to other commonly used carbon nanomaterials. Various designs of printed carbon electrodes, incorporating carbon-based nanomaterials alone or in combination with other nanomaterials, have been employed for $H_2O_2$ analysis[14-18]. However, to our knowledge, non-enzymatic sensors modified with CB and δ-FeOOH have not yet been developed.

This study presents a novel non-enzymatic sensor for accurate electrochemical detection of $H_2O_2$. The sensor utilizes a disposable electrochemical cell (DCell) with a modified working electrode consisting of CB and Ag/δ-FeOOH, significantly enhancing the electrochemical detection of $H_2O_2$. Furthermore, we evaluated the sensor performance in biological samples, demonstrating its suitability for reliable $H_2O_2$ detection.

## 2. Materials and Methods

### *2.1. Reagents and apparatus*

The chemicals used in this paper were of analytical grade and used as supplied. Ammonium iron (II) sulfate hexahydrate $(NH_4)_2Fe(SO_4)_2{\cdot}6H_2O$, sodium hydroxide (NaOH), 30% (v/v) hydrogen peroxide ($H_2O_2$) aqueous solution, silver nitrate ($AgNO_3$), sodium borohydride ($NaBH_4$), potassium hexacyanoferrate (III), potassium hexacyanoferrate (II) trihydrate, poly(diallyldimethylammonium chloride) (PDDA) (20 wt.% in $H_2O$), dopamine hydrochloride, ascorbic acid, uric acid, and disinfected fetal bovine serum (FBS) were purchased from Sigma-Aldrich (St. Louis, MO, USA ). Carbon Black powder (Grade N347) was purchased from Omsk Carbon Group (Omsk, Russian Federation). Sodium phosphate monobasic ($NaH_2PO_4$) and sodium phosphate dibasic ($Na_2HPO_4$) were obtained from Dinâmica Química (Indaiatuba, SP, Brazil), and potassium chloride (KCl), and 37% (v/v) hydrogen chloride (HCl) were supplied from Labsynth (Diadema, SP, Brazil). Ultrapure water from a Millipore Direct Q® system (Billerica, MA, USA) was used to prepare the working solutions.

Electrochemical measurements were performed using a potentiostat/galvanostat (Palmses4, model PALM-PS4F210, Palmsens) connected to a computer running PSTrace 5.9 software. The electrochemical transducer was a custom-made disposable plastic electrochemical cell (Dcell) comprising three electrodes integrated into a single strip: a carbon working electrode (WE) with an area of 0.07 $cm^2$, an Ag/AgCl reference electrode (RE), and a carbon counter electrode (CE). The fabrication of DCell followed a previously reported method involving a simple procedure utilizing a home cutter printer for prototyping and laminating[19]. The morphology of the films was assessed using scanning electron microscopy (SEM) with a DSM960 microscope (CarlZeiss, Jena, Germany) equipped with an energy-dispersive X-ray spectrometer (EDS).

Preprints (www.preprints.org) | NOT PEER-REVIEWED | Posted: 10 October 2023 doi:10.20944/preprints202310.0476.v1



*2.2. Synthesis of Ag/δ-FeOOH*

The synthesis of δ-FeOOH was carried out following a previously reported procedure [7,20]. In brief, 200 mL of 0.71 mM $(NH_4)_2Fe(SO_4)_2{\cdot}6H_2O$ solution was mixed with 200 mL of 2 M NaOH solution under mechanical agitation. After forming a green precipitate, 5 mL of 30 % $H_2O_2$ solution was added and stirred for 30 min. The aspect of a reddish-brown precipitate indicated the formation of the δ-FeOOH particles. The dispersion was thoroughly washed with water to purify the nanoparticles and dried in a vacuum desiccator at room temperature.

Ag/δ-FeOOH was prepared by adding 10 mL of 5 % (m/m) $AgNO_3$ solution to a 1.0 g of δ-FeOOH dispersion in 25 mL of water. After stirring for 15 min, the mixture was left to stand for 12 h. Subsequently, 30 mg $NaBH_4$ was added to the solution under stirring for 15 min. The Ag/δ-FeOOH nanocomposite was washed multiple times with water and dried in a vacuum desiccator at room temperature.

*2.3. Preparation of DCell-CB//Ag/δ-FeOOH*

The working electrode of the DCell was modified by applying a dispersion prepared under optimized conditions. For the preparation, 1 mL of deionized water was utilized, with the pH adjusted to 10 using a NaOH solution. The dispersion consisted of 1 mg of CB, 1 µL of PDDA, and 1 mg of Ag/δ-FeOOH. The mixture was ultrasonicated for 10 min at 30 ºC. Then, 10 µL of dispersion was drop-casted on Dcell and air-dried at room temperature (Scheme 1).

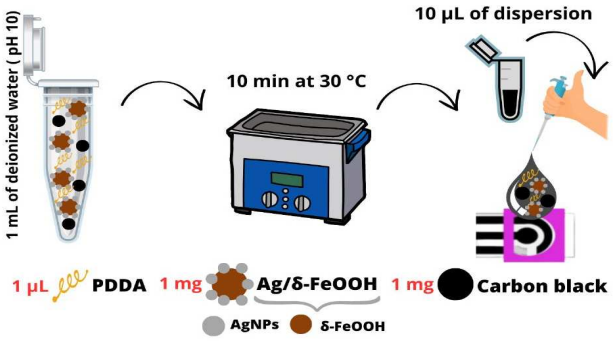


**Scheme 1.** Schematic representation of the straightforward fabrication process for DCell-CB//Ag/δ-FeOOH.

*2.4. Electrochemical characterization*

The electrochemical properties of modified and unmodified DCell were analyzed using cyclic voltammetric (CV) and electrochemical impedance spectroscopy (EIS). The tests were conducted in 1 mM of $K_3Fe(CN)_6$ and 1 mM of $K_4Fe(CN)_6$ in a 0.1 M KCl solution at pH 3.2. For the EIS measurements, an open circuit potential was applied with an amplitude of 5 mV and a frequency range of 100 kHz to 0.01 Hz. To evaluate the electrochemical sensing capabilities of the modified Dcell, CV and amperometry techniques were employed in an $N_2$-saturated 0.2 M PBS solution at pH 7.2, with or without $H_2O_2$.

## 3. Results and discussion

*3.1. Morphological and electrochemical characterization of DCell-CB//Ag/δ-FeOOH*

Figure 1A presents the SEM image of the DCell-CB//Ag/δ-FeOOH. The image reveals a well-coated mixture of CB and Ag/δ-FeOOH on the working electrode, displaying a heterogeneous surface with porous topography. Notably, the modified electrode exhibits increased surface irregularities compared to the unmodified DCell previously reported[19], which can enhance conductivity and the analytical response. EDS analysis in Figure 1B shows C, Ag, and Fe, validating the successful modification of DCell's working electrode.

EIS and CV were used to evaluate the performance of the modified and unmodified DCell in a ferri-ferro cyanide solution. Figure 2A shows EIS spectra for DCell (a), DCell modified with Ag/δ-FeOOH (b), and DCell modified with CB//Ag/δ-FeOOH (c). The bare DCell exhibited an Rct of $1.4 \times 10^4$ Ω, which significantly decreased after modification with Ag/δ-FeOOH (389 Ω) and CB//Ag/δ-FeOOH

Preprints (www.preprints.org) | NOT PEER-REVIEWED | Posted: 10 October 2023 doi:10.20944/preprints202310.0476.v1



(130 Ω). These findings indicate that Ag/δ-FeOOH and CB//Ag/δ-FeOOH play a crucial role as promoters of electron transfer in the ferri/ferro-cyanide redox system at the working electrode surface. The CV results in Figure 2B align well with the EIS findings. DCell-CB//Ag/δ-FeOOH demonstrated better current response ($I_{oxi}$ = 38.10 μA and $I_{red}$ = -36.31 μA, ΔEp = 110 mV) compared to DCell-Ag/δ-FeOOH ($I_{oxi}$ = 18.83 μA and $I_{red}$ = -23.22 μA, ΔEp = 110 mV) and bare DCell ($I_{oxi}$ = 7.01 μA and $I_{red}$ = -7.01 μA, ΔEp = 270 mV). The ΔEp value of more than 58 mV (the expected value for one-electron Nernstian-precess) suggests a quasi-reversible electrochemical response. The significant improvement observed can be attributed to the specific properties of CB, such as high surface area and excellent conductivity[13]. Previous studies have reported that screen-printed electrodes modified with CB by drop-casting exhibit lower peak-to-peak separation and higher intensity peak current in a ferri-ferro cyanide solution, aligning with our findings[13,21].

Furthermore, the magnitudes of the voltammetric peak currents plotted against the square root of the applied scan rate ($\upsilon^{1/2}$) ranging from 10 – 200 mV $s^{-1}$, exhibited a linear relationship for the bare DCell, DCell-Ag/δ-FeOOH, and DCell-CB//Ag/δ-FeOOH, indicating a diffusion-controlled process at the electrode surface (Figure SI 1). The apparent heterogeneous electron-transfer rate constant, $K^0_{app}$, for the quasi-reversible system was determined using the Nicholson method[22-24]. The rate constants calculated in the ferri-ferro cyanide solution were 3.21 x $10^{-4}$±9.36 x $10^{-6}$ cm $s^{-1}$, 1.66 x $10^{-3}$±6.10 x $10^{-5}$ cm $s^{-1}$, and 3.06 x $10^{-3}$±1.10 x $10^{-4}$ cm $s^{-1}$, for the bare Dcell, DCell-Ag/δ-FeOOH, and DCell-CB//Ag/δ-FeOOH, respectively. These results demonstrate that DCell-CB//Ag/δ-FeOOH exhibits superior performance, with a rate constant almost twice that of DCell-Ag/δ-FeOOH. The slower electron transfer rate observed for the bare DCell in the ferri-ferro cyanide solution is consistent with the higher Rct value obtained from the EIS data. Our experimental findings indicate significant improvements in the electrochemical performance of DCell-CB//Ag/δ-FeOOH using CB, highlighting the advantages of incorporating CB to enhance the magnitude of $K^0_{app}$ [13].

Additionally, the working electrodes areas for bare DCell, DCell-Ag/δ-FeOOH, and DCell-CB//Ag/δ-FeOOH were determined experimentally using the Randles-Sevčík equation[19,25]. The electroactive areas, evaluated using the ferri-ferro cyanide solution, were found to be 0.021±0.002 $cm^2$, 0.190±0.010 $cm^2$, and 0.239±0.009 $cm^2$, respectively. The DCell modified with CB and Ag/δ-FeOOH exhibited a larger electroactive area, providing more sites for electrochemical reactions, consistent with the superior electrochemical behavior observed for DCell-CB//Ag/δ-FeOOH.

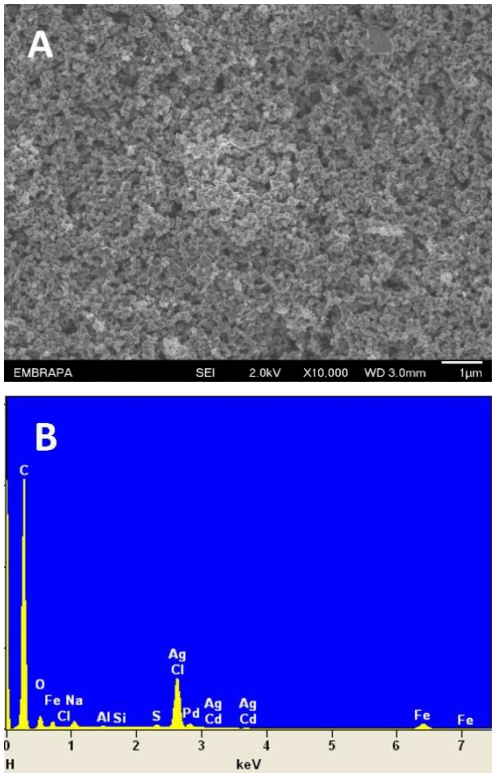


**Figure 1.** A. SEM images and B. EDS spectrum of DCell modified with CB//Ag/δ-FeOOH.

Preprints (www.preprints.org) | NOT PEER-REVIEWED | Posted: 10 October 2023 doi:10.20944/preprints202310.0476.v1



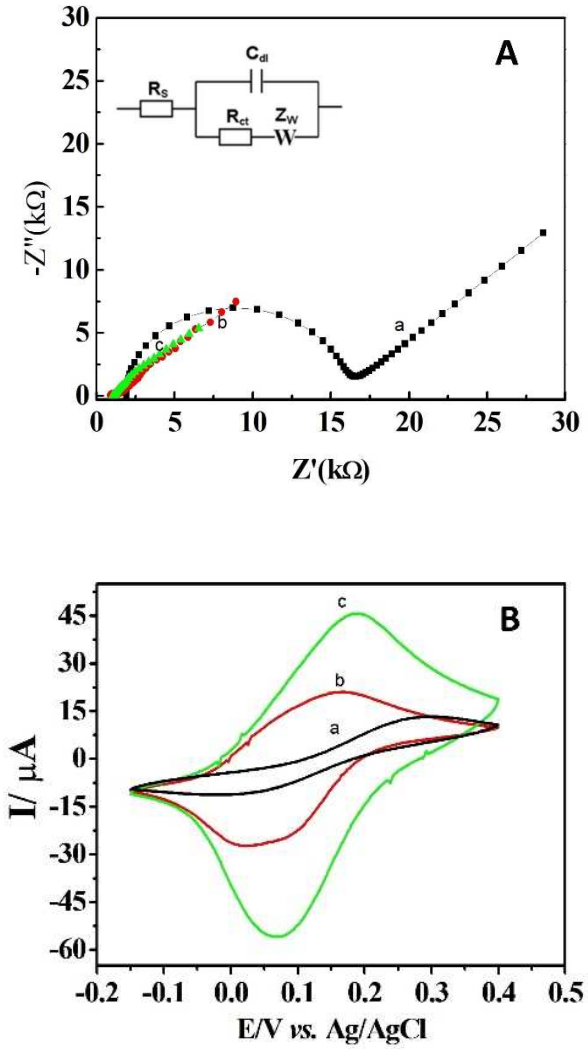


**Figure 2.** A. Impedance plots at open-circuit potential and B. Cyclic voltammograms at 100mV $s^{-1}$ using 1 mM $K_3Fe(CN)_6$ and 1 mM $K_4Fe(CN)_6$ in 0.1 M KCl pH 3.2 for (a) Dcell, (b) DCell modified with Ag/δ-FeOOH, and (c) DCell modified with CB//Ag/δ-FeOOH.

*3.2. Electrochemical behavior of $H_2O_2$ in DCell-CB//Ag/δ-FeOOH*

Cyclic voltammetry (CV) was utilized to inquire the electrochemical characteristics of DCell-CB//Ag/δ-FeOOH for $H_2O_2$ reduction. The voltammograms of DCell (a), DCell – CB (b), DCell - CB//δ-FeOOH (c), and DCell – CB//Ag/δ-FeOOH (d) in $N_2$-saturated 0.2 M PBS at pH 7.2 with 500 μM of $H_2O_2$, recorded at a scan rate of 100 mV $s^{-1}$, are presented in Figure 3A. Curves a and b show no distinct response to $H_2O_2$ in the -1.0 to 1.0 V range for DCell and DCell-CB, respectively. Curve c, corresponding to DCell - CB//δ-FeOOH, demonstrates an anodic current of 16μA, and a cathodic current of 19 μA at -0.15V and -0.75 V, respectively, in the presence of $H_2O_2$, indicating the redox process of $H_2O_2$ on δ-FeOOH[7]. Curve d, representing the electrochemical profile of DCell-CB//Ag/δ-FeOOH in $H_2O_2$ solution, displays an anodic current of 134.0 μA and 39.4 μA at 0.08V and –0.15 V, respectively, as well as a cathodic current of 100.0 μA and 57.0 μA at -0.3V and -0.75V, respectively.

The sharp oxidation peak at 0.08 V can be assigned to the oxidation of silver nanoparticles coverage on δ-FeOOH, and the reduction peak at -0.3 V may arise from the reduction of silver halides or silver oxide formed during the forward scan on δ-FeOOH. Similar observations were reported by Plowman et al. for gold-silver alloy nanoparticles in KCl solution, where an oxidation peak of silver nanoparticles at 0.14 V and a reduction peak at 0.01 V in the reverse scan were attributed to the

Preprints (www.preprints.org) | NOT PEER-REVIEWED | Posted: 10 October 2023 doi:10.20944/preprints202310.0476.v1



reduction of silver chloride formed in the forward scan[26]. The peak currents at -0.15 V and -0.75V can be attributed to the redox process of $H_2O_2$ on CB//Ag/δ-FeOOH.

Figure 3B illustrates the voltammograms of DCell–Ag/δ-FeOOH (a) and DCell–CB//Ag/δ-FeOOH (b) along with their respective background voltammograms in $N_2$-saturated 0.2 M PBS at pH 7.2, with and without 500 μM $H_2O_2$, recorded at a scan rate of 100 mV $s^{-1}$. Notably, CB on the working electrode catalyzes the redox process of silver on δ-FeOOH in PBS, leading to anodic and cathodic peaks at 0.08 V and -0.3 V, respectively, which are absent in the voltammogram of DCell–Ag/δ-FeOOH. Furthermore, a 33% increase in the cathodic peak current at -0.75 V in 500 μM $H_2O_2$/ PBS solution is observed for DCell–CB//Ag/δ-FeOOH compared to DCell–Ag/δ-FeOOH. These results can be assigned to the superior electrochemical behavior and higher electroactive area of the working electrode in DCell-CB//Ag/ δ-FeOOH. The enhancement of electroanalytical performance for $H_2O_2$ observed in working electrodes modified with CB has been reported in previous studies, indicating improved electrochemical activity due to the high conductivity and large specific surface area provided by CB[27,28].

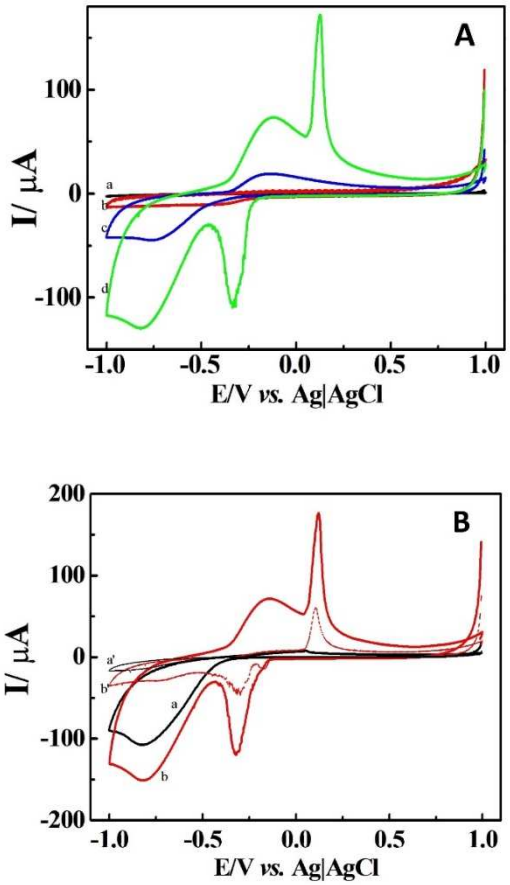


**Figure 3.** A. Cyclic voltammograms of DCell (a), DCell–CB (b), DCell-CB//δ-FeOOH (c), and DCell–CB//Ag/δ-FeOOH (d) and B. Cyclic voltammograms of DCell–Ag/δ-FeOOH (a) and DCell–CB//Ag/δ-FeOOH (b) in $N_2$-saturated 0.2 M PBS at pH 7.2 with 500 μM $H_2O_2$ at a scan rate of 100 $mVs^{-1}$. a′ and b′ represents the background voltammograms.

After confirming that DCell-CB//Ag/δ-FeOOH exhibited the best electrochemical characteristic for $H_2O_2$ detection, we investigated the peak potential of cyclic voltammetry for detecting $H_2O_2$ at different concentrations. Amperometry measurements were conducted in $N_2$-saturated 0.2 M PBS at pH 7.2, under magnetic agitation, using $H_2O_2$ concentrations of 100, 500, and 1000 μM. As shown in Figure 4, an increase in current is observed at -0.75 V with increasing $H_2O_2$ concentration. However, no significant changes in current were observed at -0.3 V, -0.15 V, and 0.08V, indicating the absence of an electrochemical process for $H_2O_2$ at those potentials. Consequently, these potentials were not

Preprints (www.preprints.org) | NOT PEER-REVIEWED | Posted: 10 October 2023 doi:10.20944/preprints202310.0476.v1



effective for electroanalysis. Considering the maximum current achieved at -0.75 V, we selected -0.75 V as the potential for $H_2O_2$ detection using DCell-CB//Ag/ δ-FeOOH.

Figure 5A depicts the amperometry response of DCell-CB//Ag/δ-FeOOH at -0.75V for $H_2O_2$ detection in $N_2$-saturated 0.2 M PBS (pH 7.2) under continuous stirring. The response of DCell-CB//Ag/δ-FeOOH for $H_2O_2$ reduction is rapid, reaching a steady-state signal quickly upon $H_2O_2$ addition. As shown in Figure 5B, the current changes linearly with increasing $H_2O_2$ concentration from 70 μM to 6000 μM. Typically, the concentration of $H_2O_2$ in a human cell is less than 10 nM, and in human plasma, it ranges from 1 to 5 μM. However, during inflammation, the $H_2O_2$ concentration in plasma can exceed 50 μM[29,30]. In our experiments, the limit of detection (LOD) was calculated to be 22 μM (S/N = 3), which reliably covers the concentration range in plasma during inflammation. The sensitivity of the method was 214 μA $mM^{-1}$ $cm^{-2}$. Our results demonstrate that the proposed electroanalytical method exhibits comparable features to those previously reported (see Table SI1).

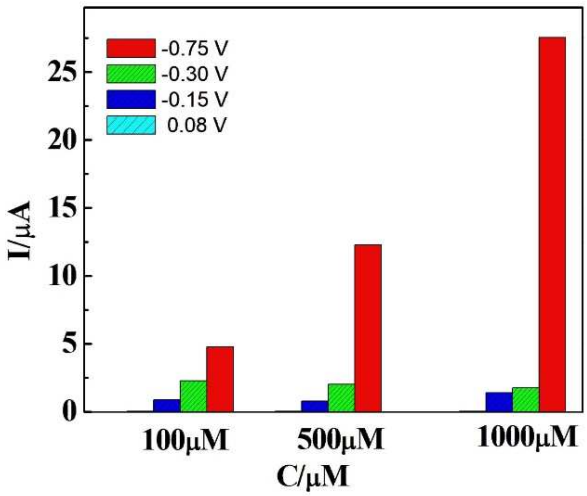


**Figure 4.** Amperometric responses of Dcell–CB//Ag/δ-FeOOH in N2-saturated 0.2 M PBS solution (pH 7.2) with 100 μM, 500 μM or 1000 μM of $H_2O_2$ at different applied potentials versus Ag|AgCl under magnetic agitation.

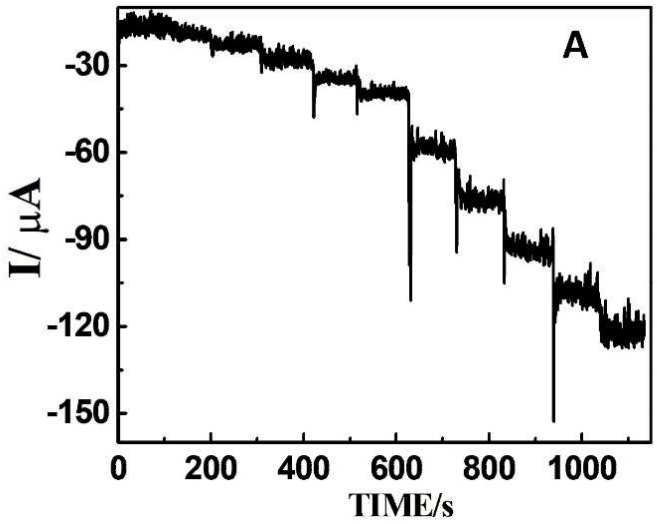

Preprints (www.preprints.org) | NOT PEER-REVIEWED | Posted: 10 October 2023 doi:10.20944/preprints202310.0476.v1



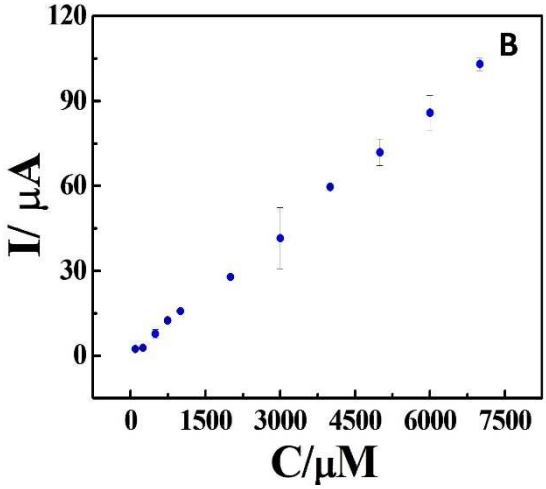


**Figure 5.** A. Amperometric responses of Dcell–CB//Ag/δ-FeOOH to successive additions of $H_2O_2$ in $N_2$-saturated 0.2 M PBS at pH 7.2 solution, recorded at an applied potential of -0.75V versus Ag|AgCl under magnetic agitation. B. Calibration curve for the amperometric determination of $H_2O_2$ concentration. The error bars show the standard deviation for N=3.

*3.4. Repeatability, Interference Studies, and Biological Sample Analysis*

We assessed the performance of DCell-CB//Ag/δ-FeOOH in generating consistent electrochemical results in PBS containing $H_2O_2$. The estimated relative standard deviation (RSD) for five independent DCell-CB//Ag/δ-FeOOH measurements was approximately 4.78%, demonstrating the reliability of the process fabrication. Furthermore, we evaluated the interference effects of common biomolecules in physiologic samples, such as ascorbic acid, uric acid, and dopamine[31,32], on DCell-CB//Ag/δ-FeOOH. Electrochemical measurements (Figure 6) were carried out in $N_2$-saturated 0.2 M PBS (pH 7.2) at -0.75V under continuous stirring. DCell-CB//Ag/δ-FeOOH displayed no amperometric signal in 100 μM of dopamine, uric acid, or ascorbic acid. However, significant amperometric responses were observed upon adding 100 μM of $H_2O_2$ in the initial and final steps. Importantly, there was no change in the current signal of $H_2O_2$ after introducing interfering agents, indicating excellent selectivity of the proposed sensor. These characteristics, coupled with the reliable response of the DCell-CB//Ag/δ-FeOOH, make it suitable for detecting $H_2O_2$ levels in biological samples.

Fetal bovine serum (FBS) is commonly added as a supplement to the basal medium in cell culture. Cells can release $H_2O_2$ when stimulated in a cell culture medium containing 10% fetal bovine serum[33,34]. Therefore, for application in biological samples, it assesses its performance in a solution containing FBS. To this end, we applied DCell-CB//Ag/δ-FeOOH to determine $H_2O_2$ levels in a 10% fetal bovine serum disinfected solution diluted in 0.2 M PBS (pH 7.2). The samples were spiked with different concentrations of $H_2O_2$ standard solution (Table 1). The calculated $H_2O_2$ recoveries fell within the range of 92 to 103%. These results highlight the potential of DCell-CB//Ag/δ-FeOOH for monitoring $H_2O_2$ in biological samples.

Preprints (www.preprints.org) | NOT PEER-REVIEWED | Posted: 10 October 2023 doi:10.20944/preprints202310.0476.v1



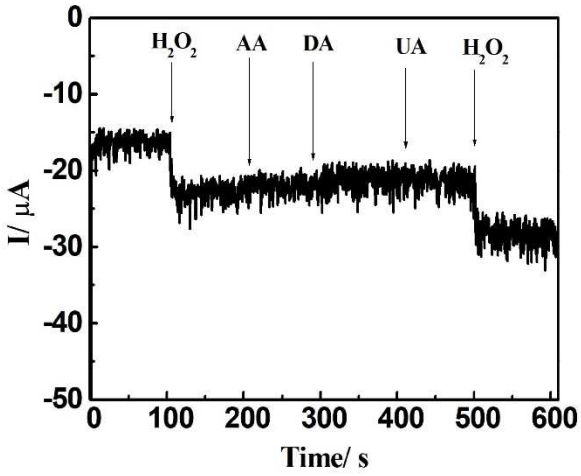


**Figure 6.** Amperometric response of Dcell – CB//Ag/δ-FeOOH using 100 μM $H_2O_2$ (initial and final additions) and 100 μM of ascorbic acid (AA), dopamine (DA), uric acid (UA) using in N2-saturated 0.2 PBS at pH 7.2, recorded at -0.75 V versus Ag|AgCl under continuous stirring.

**Table 1.** Spiked and recovery of $H_2O_2$ in 10% of fetal bovine serum diluted in PBS.

| Sample | Added (μM) | Found (μM) | Recovery (μM) |
|---|---|---|---|
| 1 | 500 | 515.6 | 103% |
| 2 | 2000 | 1834.5 | 92% |

## 4. Conclusions

We developed a non-enzymatic sensor using a carbon black (CB) and Ag/δ-FeOOH composite for $H_2O_2$ detection. The effective immobilization of the CB and Ag/δ-FeOOH composite onto the DCell working electrode was confirmed through SEM, EDS, and EIS analyses. The incorporation of CB into the DCell-CB//Ag/δ-FeOOH sensor resulted in a significant improvement in its electrochemical performance, leveraging the unique properties of CB. Specifically, the apparent rate constant of heterogeneous electron transfer in DCell-CB//Ag/δ-FeOOH was nearly doubled compared to that of DCell–Ag/δ-FeOOH. Our sensor demonstrated exceptional sensitivity, reproducibility, and selectivity for electrochemical $H_2O_2$ detection. Furthermore, the successful application of the sensor in the electroanalytical assay of 10% fetal bovine serum highlighted its potential for precise $H_2O_2$ detection in complex biological samples. These findings emphasize the promising prospects of the DCell-CB//Ag/δ-FeOOH sensor in advancing electrochemical sensing technologies for diverse biomedical and environmental applications.

**Supplementary Materials:** The following supporting information can be downloaded at the website of this paper posted on Preprints.org.

**Author Contributions:** WER: Conceptualization, Methodology, Experimental work, Data Analysis, and Writing – original draft. KSN and ALHKF: Methodology and Experimental work. MCP: Resource and Writing – review and editing. LHCM and RCF: Methodology, Experimental work and Resource. ASA: Conceptualization, Supervision, Methodology, Data Analysis, Resource and Writing – review and editing.

**Acknowledgments:** We thank FAPEMIG (grant, APQ-00607-22), CNPq, and FINEP/MCTI for their support. We also acknowledge the Institute of Science, Engineering, and Technology of the Federal University of Jequitinhonha and Mucuri Valleys for supporting this work.

**Conflicts of Interest:** The authors declare no conflict of interest.

## References

1. Berg, D. Biomarkers for the early detection of Parkinson's and Alzheimer's disease. *Neurodegener. Dis.* **2008**, *5*, 133-136, doi:10.1159/000113682.
2. Pepe, M.S.; Etzioni, R.; Feng, Z.D.; Potter, J.D.; Thompson, M.L.; Thornquist, M.; Winget, M.; Yasui, Y. Phases of biomarker development for early detection of cancer. *J. Natl. Cancer Inst.* **2001**, *93*, 1054-1061, doi:10.1093/jnci/93.14.1054.
3. Deshpande, A.S.; Muraoka, W.; Andreescu, S. Electrochemical sensors for oxidative stress monitoring. *Curr. Opin. Electrochem.* **2021**, *29*, 10, doi:10.1016/j.coelec.2021.100809.
4. Geraskevich, A.V.; Solomonenko, A.N.; Dorozhko, E.V.; Korotkova, E.I.; Barek, J. Electrochemical Sensors for the Detection of Reactive Oxygen Species in Biological Systems: A Critical Review. *Crit. Rev. Anal. Chem.* **2022**, 33, doi:10.1080/10408347.2022.2098669.
5. Chen, X.M.; Wu, G.H.; Cai, Z.X.; Oyama, M.; Chen, X. Advances in enzyme-free electrochemical sensors for hydrogen peroxide, glucose, and uric acid. *Microchim. Acta* **2014**, *181*, 689-705, doi:10.1007/s00604-013-1098-0.
6. Thatikayala, D.; Ponnamma, D.; Sadasivuni, K.K.; Cabibihan, J.J.; Al-Ali, A.K.; Malik, R.A.; Min, B. Progress of Advanced Nanomaterials in the Non-Enzymatic Electrochemical Sensing of Glucose and $H_2O_2$. *Biosensors-Basel* **2020**, *10*, 34, doi:10.3390/bios10110151.
7. de Meira, F.H.A.; Resende, S.F.; Monteiro, D.S.; Pereira, M.C.; Mattoso, L.H.C.; Faria, R.C.; Afonso, A.S. A Non-enzymatic Ag/delta-FeOOH Sensor for Hydrogen Peroxide Determination using Disposable Carbon-based Electrochemical Cells. *ELECTROANALYSIS* **2020**, *32*, 2231-2236, doi:10.1002/elan.202060171.
8. Huang, Z.X.; Han, F.S.; Li, M.T.; Zhou, Z.H.; Guan, X.J.; Guo, L.J. Which phase of iron oxyhydroxides (FeOOH) is more competent in overall water splitting as a photocatalyst, goethite, akaganeite or lepidocrocite? A DFT-based investigation. *Comput. Mater. Sci.* **2019**, *169*, 8, doi:10.1016/j.commatsci.2019.109110.
9. Zhang, N.; Sheng, Q.L.; Zhou, Y.Z.; Dong, S.Y.; Zheng, J.B. Synthesis of FeOOH@PDA-Ag nanocomposites and their application for electrochemical sensing of hydrogen peroxide. *J. Electroanal. Chem.* **2016**, *781*, 315-321, doi:10.1016/j.jelechem.2016.07.012.
10. Zhang, J.; Zheng, J.B. An enzyme-free hydrogen peroxide sensor based on Ag/FeOOH nanocomposites. *Analytical Methods* **2015**, *7*, 1788-1793, doi:10.1039/c4ay02881c.
11. Zhao, C.L.; Zhang, H.F.; Zheng, J.B. Synthesis of silver decorated sea urchin-like FeOOH nanocomposites and its application for electrochemical detection of hydrogen peroxide. *J. Mater. Sci.-Mater. Electron.* **2017**, *28*, 14369-14376, doi:10.1007/s10854-017-7297-4.
12. Huang, Y.L.; Liang, G.Z.; Lin, T.R.; Hou, L.; Ye, F.G.; Zhao, S.L. Magnetic Cu/Fe3O4@FeOOH with intrinsic HRP-like activity at nearly neutral pH for one-step biosensing. *Anal. Bioanal. Chem.* **2019**, *411*, 3801-3810, doi:10.1007/s00216-019-01841-y.
13. Arduini, F.; Cinti, S.; Mazzaracchio, V.; Scognamiglio, V.; Amine, A.; Moscone, D. Carbon black as an outstanding and affordable nanomaterial for electrochemical (bio)sensor design. *Biosens. Bioelectron.* **2020**, *156*, 16, doi:10.1016/j.bios.2020.112033.
14. Cinti, S.; Arduini, F. Graphene-based screen-printed electrochemical (bio)sensors and their applications: Efforts and criticisms. *Biosens. Bioelectron.* **2017**, *89*, 107-122, doi:10.1016/j.bios.2016.07.005.
15. Ahmad, K.; Kim, H. Fabrication of Nitrogen-Doped Reduced Graphene Oxide Modified Screen Printed Carbon Electrode (N-rGO/SPCE) as Hydrogen Peroxide Sensor. *Nanomaterials* **2022**, *12*, 14, doi:10.3390/nano12142443.
16. He, G.W.; Jiang, J.Q.; Wu, D.; You, Y.L.; Yang, X.; Wu, F.; Hu, Y.J. A Novel Nonenzymatic Hydrogen Peroxide Electrochemical Sensor Based on Facile Synthesis of Copper Oxide Nanoparticles Dopping into Graphene Sheets@Cerium Oxide Nanocomposites Sensitized Screen Printed Electrode. *Int. J. Electrochem. Sci.* **2016**, *11*, 8486-8498, doi:10.20964/2016.10.34.
17. Hu, Y.; Hojamberdiev, M.; Geng, D.S. Recent advances in enzyme-free electrochemical hydrogen peroxide sensors based on carbon hybrid nanocomposites. *J. Mater. Chem. C* **2021**, *9*, 6970-6990, doi:10.1039/d1tc01053k.
18. Yang, X.; Ouyang, Y.J.; Wu, F.; Hu, Y.J.; Zhang, H.F.; Wu, Z.Y. In situ & controlled preparation of platinum nanoparticles dopping into graphene sheets@cerium oxide nanocomposites sensitized screen printed electrode for nonenzymatic electrochemical sensing of hydrogen peroxide. *J. Electroanal. Chem.* **2016**, *777*, 85-91, doi:10.1016/j.jelechem.2016.08.008.
19. Afonso, A.S.; Uliana, C.V.; Martucci, D.H.; Faria, R.C. Simple and rapid fabrication of disposable carbon-based electrochemical cells using an electronic craft cutter for sensor and biosensor applications. *Talanta* **2016**, *146*, 381-387, doi:10.1016/j.talanta.2015.09.002.
20. Pereira, M.C.; Garcia, E.M.; da Silva, A.C.; Lorencon, E.; Ardisson, J.D.; Murad, E.; Fabris, J.D.; Matencio, T.; Ramalho, T.D.; Rocha, M.V.J. Nanostructured delta-FeOOH: a novel photocatalyst for water splitting. *Journal of Materials Chemistry* **2011**, *21*, 10280-10282, doi:10.1039/c1jm11736j.
21. Arduini, F.; Di Nardo, F.; Amine, A.; Micheli, L.; Palleschi, G.; Moscone, D. Carbon Black-Modified Screen-Printed Electrodes as Electroanalytical Tools. *Electroanalysis* **2012**, *24*, 743-751, doi:10.1002/elan.201100561.

22. Nicholson, R.S. THEORY AND APPLICATION OF CYCLIC VOLTAMMETRY FOR MEASUREMENT OF ELECTRODE REACTION KINETICS. *Anal. Chem.* **1965**, *37*, 1351-+, doi:10.1021/ac60230a016.
23. Moore, K.E.; Flavel, B.S.; Ellis, A.V.; Shapter, J.G. Comparison of double-walled with single-walled carbon nanotube electrodes by electrochemistry. *Carbon* **2011**, *49*, 2639-2647, doi:10.1016/j.carbon.2011.02.048.
24. Muhammad, H.; Tahiri, I.A.; Muhammad, M.; Masood, Z.; Versiani, M.A.; Khaliq, O.; Latif, M.; Hanif, M. A comprehensive heterogeneous electron transfer rate constant evaluation of dissolved oxygen in DMSO at glassy carbon electrode measured by different electrochemical methods. *J. Electroanal. Chem.* **2016**, *775*, 157-162, doi:10.1016/j.jelechem.2016.05.049.
25. Paixao, T. Measuring Electrochemical Surface Area of Nanomaterials versus the Randles-Sevcik Equation. *Chemelectrochem* **2020**, *7*, 3414-3415, doi:10.1002/celc.202000633.
26. Plowman, B.J.; Sidhureddy, B.; Sokolov, S.V.; Young, N.P.; Chen, A.C.; Compton, R.G. Electrochemical Behavior of Gold-Silver Alloy Nanoparticles. *Chemelectrochem* **2016**, *3*, 1039-1043, doi:10.1002/celc.201600212.
27. Faisal, M.; Alam, M.M.; Asiri, A.M.; Alsaiari, M.; Alruwais, R.S.; Jalalah, M.; Madkhali, O.; Rahman, M.M.; Harraz, F.A. Detection of hydrogen peroxide with low-dimensional silver nanoparticle-decorated PPy-C/TiO2 nanocomposites by electrochemical approach. *J. Electroanal. Chem.* **2023**, *928*, 11, doi:10.1016/j.jelechem.2022.117030.
28. Liu, Y.Y.; Li, H.M.; Gong, S.P.; Chen, Y.N.; Xie, R.R.; Wu, Q.Q.; Tao, J.; Meng, F.L.; Zhao, P. A novel non-enzymatic electrochemical biosensor based on the nanohybrid of bimetallic PdCu nanoparticles/carbon black for highly sensitive detection of H2O2 released from living cells. *Sens. Actuator B-Chem.* **2019**, *290*, 249-257, doi:10.1016/j.snb.2019.03.129.
29. Forman, H.J.; Bernardo, A.; Davies, K.J.A. What is the concentration of hydrogen peroxide in blood and plasma? *Arch. Biochem. Biophys.* **2016**, *603*, 48-53, doi:10.1016/j.abb.2016.05.005.
30. Wang, Z.; Hong, Y.L.; Li, J.B.; Liu, J.L.; Jiang, H.; Sun, L.N. Upconversion luminescent sensor for endogenous H2O2 detection in cells based on the inner filter effect of coated silver layer. *Sens. Actuator B-Chem.* **2023**, *376*, 8, doi:10.1016/j.snb.2022.132936.
31. Chakraborty, P.; Dhar, S.; Debnath, K.; Majumder, T.; Mondal, S.P. Non-enzymatic and non-invasive glucose detection using Au nanoparticle decorated CuO nanorods. *Sens. Actuator B-Chem.* **2019**, *283*, 776-785, doi:10.1016/j.snb.2018.12.086.
32. Waldiya, M.; Bhagat, D.; Narasimman, R.; Singh, S.; Kumar, A.; Ray, A.; Mukhopadhyay, I. Development of highly sensitive H2O2 redox sensor from electrodeposited tellurium nanoparticles using ionic liquid. *Biosens. Bioelectron.* **2019**, *132*, 319-325, doi:10.1016/j.bios.2019.02.050.
33. Mao, X.X.; Liu, S.W.; Su, B.Y.; Wang, D.J.; Huang, Z.; Li, J.; Zhang, Y.G. Luminescent europium(III)-organic framework for visual and on-site detection of hydrogen peroxide via a tablet computer. *Microchim. Acta* **2020**, *187*, 11, doi:10.1007/s00604-020-04379-4.
34. van der Valk, J. Fetal bovine serum-a cell culture dilemma. *Science* **2022**, *375*, 143-144, doi:10.1126/science.abm1317.